Scale for the Phase Diagram of Quantum Chromodynamics

Sourendu Gupta, *et al.*

Science **332**, 1525 (2011);
DOI: 10.1126/science.1204621

CORRECTED 16 SEPTEMBER 2011; SEE LAST PAGE

Scale for the Phase Diagram of Quantum Chromodynamics

Sourendu Gupta,[1] Xiaofeng Luo,[2,3] Bedangadas Mohanty,[4*] Hans Georg Ritter,[3] Nu Xu[5,3]

Matter described by quantum chromodynamics (QCD), the theory of strong interactions, may undergo phase transitions when its temperature and the chemical potentials are varied. QCD at finite temperature is studied in the laboratory by colliding heavy ions at varying beam energies. We present a test of QCD in the nonperturbative domain through a comparison of thermodynamic fluctuations predicted in lattice computations with the experimental data of baryon number distributions in high-energy heavy ion collisions. This study provides evidence for thermalization in these collisions and allows us to find the crossover temperature between normal nuclear matter and a deconfined phase called the quark gluon plasma. This value allows us to set a scale for the phase diagram of QCD.

Quantum chromodynamics (QCD) is the theory of strong interactions—one of the four fundamental interactions occurring in nature and an essential part of the standard model of particle physics. It describes interactions between quarks and gluons, which are the ultimate constituents of the majority of the visible mass of the universe (*1*, *2*). In the short-distance regime in which the momentum exchange between quarks and gluons is large, the strong coupling constant becomes small through the mechanism of asymptotic freedom. In this perturbative region, QCD is very successful in explaining various processes observed in experiments involving electron-positron, proton-proton, and proton-antiproton collisions (*3*). In the nonperturbative regime, tests of the theory were related to the computation of hadron properties (*4*). In other regimes of long-distance nonperturbative physics, the theory is yet to be tested. Here, we test the thermodynamics of bulk strongly interacting matter.

Experimental tests of nonperturbative QCD in the bulk can be carried out by colliding heavy ions (such as U, Pb, Au, and Cu) at different center-of-mass energies, $\sqrt{s_{NN}}$ (*5*–*8*). Several experimental programs have been launched or are in the planning stage at facilities such as the Large Hadron Collider (LHC), the Relativistic Heavy Ion Collider (RHIC), the Super Proton Synchrotron (SPS), the Facility for Anti-proton and Ion Research (FAIR), and the Nuclotron-based Ion Collider fAcility (NICA), where the essential features of the QCD phase diagram can be studied.

In QCD, there are conserved quantities such as the net-baryon number B, the net-electric charge Q, and the net-strangeness S. The term "net" means the algebraic sum of the quantum numbers, where those of anti-particles are the negatives of the corresponding particles. As a result, the thermodynamics of the bulk can be characterized by the corresponding chemical potentials (energy needed to add or remove one unit of the conserved quantity to or from the system, respectively) μ_B, μ_Q, and μ_S in addition to the temperature T, conjugate to the conserved energy of a bulk system. In experimental studies of particle ratios measured in heavy-ion collisions, it is observed that the relevant values of μ_Q and μ_S are small compared with μ_B. For example, in Au ion collisions within rapidity range of ±0.1 unit at $\sqrt{s_{NN}}$ = 200 GeV (with impact parameter less than 3 fm) one finds that $\mu_B = 22 \pm 4.5$ MeV, whereas $\mu_S = 3.9 \pm 2.6$ MeV, and μ_Q is still smaller (*9*).

The lattice formulation of QCD is a nonperturbative approach from first principles for obtaining the predictions of QCD. Space-time is replaced by a lattice; quarks occupy the sites, and gluons occupy the links between the sites. The lattice spacing a is the inverse of the cutoff required to regulate any interacting quantum field theory. The theory is solved numerically at several values of a. The extrapolation to the continuum ($a = 0$) can then be made through the renormalization group equations. In QCD, there is a conventional temperature, T_c, that is an intrinsic scale of bulk hadronic matter. We follow the definition that it is the temperature at the peak of a susceptibility related to the confinement-deconfinement order parameter (called the Polyakov loop susceptibility, χ_L) at $\mu_B = 0$ (*10*–*13*). Lattice QCD computations show that this peak is finite, which corresponds to a crossover (*14*, *15*). The temperature at which χ_L peaks, of course, changes with μ_B. However, once T_c is known such shifts as a function of μ_B can be quantified. This is similar to saying that the Celsius scale of temperature is defined by the boiling point of water at normal pressure P, and that the boiling point changes with P.

One of the most basic questions to ask about bulk hadronic matter is the value of T_c. This can be represented as a link in a "circle of reasoning" that encompasses all the regimes of nonperturbative QCD (Fig. 1). So far, the strategy to find T_c has been indirect: First, lattice QCD computations are performed at both $T = 0$ and $T > 0$ in order to determine a ratio T_c/m, where m is a typical hadronic scale [Fig. 1, step (b)]. Then one replaces the scale m, determined on the lattice, with an experimental measurement [Fig. 1, step (a)]. The temperature at each $\sqrt{s_{NN}}$ extracted from models of particle yields (*16*, *17*) is step (d) of the circle of reasoning. From such models, one finds that the fireball of bulk nuclear matter created in heavy ion collisions, which is initially out of equilibrium, evolves to a state of thermal equilibrium at chemical freeze-out. The models do not give T_c; however, they allow the extraction of T and μ_B at freeze-out. We show that predictions

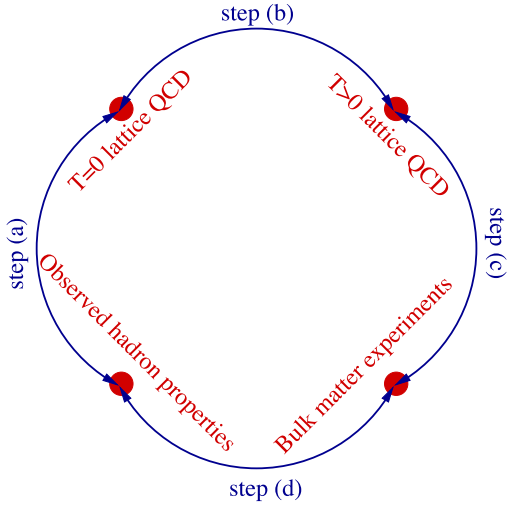

Fig. 1. Illustration of the chain of reasoning for testing QCD in the nonperturbative domains of the strong interactions and obtaining the scale, T_c, of the QCD phase diagram.

[1]Department of Theoretical Physics, Tata Institute of Fundamental Research, Homi Bhabha Road, Mumbai 400005, India. [2]Department of Modern Physics, University of Science and Technology of China, Hefei 230026, China. [3]Nuclear Science Division, Lawrence Berkeley National Laboratory, Berkeley, CA 94720, USA. [4]Experimental High Energy Physics and Applications Group, Variable Energy Cyclotron Centre, 1/AF Bidhan Nagar, Kolkata 700064, India. [5]College of Physical Science and Technology, Central China Normal University, Wuhan 430079, China.

*To whom correspondence should be addressed. E-mail: bedanga@vecc.gov.in

of lattice computations of finite temperature QCD (*18*), taken in conjunction with determinations of T_c in step (b) (*10*–*13*), agree well with experimental measurements on bulk hadronic matter (*19*). This allows us to invert the reasoning and extract T_c directly from the experimental measurements in heavy ion collisions [Fig. 1, step (c)]. The agreement of the temperature from steps (c) and (d) along with the agreement of T_c extracted from steps (a) and (b) with that from (c) show the complete compatibility of a single theory of hadron properties and of bulk QCD matter, that is, of all nonperturbative regimes of the strong interactions. This approach may present a new domain of tests of the standard model of particle physics.

The conjectured phase diagram of QCD. In the current conjectures for the parts of the phase diagram that is accessible with heavy ion collisions (Fig. 2) (*20*), calculations within simplified models that mimic QCD show that at large μ_B there is a first-order hadron–quark–gluon plasma (QGP) phase transition. This phase boundary is expected to end in a critical point at finite μ_B because lattice computations (*10*–*13*) agree with general symmetry arguments (*21*), which indicate that at $\mu_B = 0$ there is neither a first-order nor a second-order phase transition but only a crossover at T_c. The determination of T_c sets the scale of the QCD phase diagram. Current best estimates of the position of the critical point (*22*) are reflected in the position indicated in Fig. 2. Currently, the experimental focus is on an attempt to locate the critical point and the line of phase coexistence (*23*, *24*).

By changing $\sqrt{s_{NN}}$, one traces out a line of chemical freeze-out in the phase diagram, as shown in Fig. 2. This line is parameterized through a hadron resonance gas model (*16*, *17*). Because this work focuses on making a connection between QCD thermodynamic calculations and observables measured in experimental facilities, we also show in Fig. 2 the range of μ_B values covered by various experiments as one traverses the chemical freeze-out line by changing $\sqrt{s_{NN}}$. The solid point around μ_B = 938 MeV is the location of ordinary nuclear matter (*25*), the best characterized point on the phase diagram.

Comparison of experimental measurements with lattice QCD predictions. Lattice QCD computations leave open the question of a scale and yield dimensionless predictions—for example, for P/T^4 as a function of T/T_c and μ_B/T. Here, we discuss the nonlinear susceptibilities (NLSs) of baryons, $\chi_B^{(n)}$, of order n (*26*). These are the Taylor coefficients in the expansion of P with respect to μ_B at fixed T in the usual dimensionless form

$$T^{n-4}\chi_B^{(n)}\left(\frac{T}{T_c},\frac{\mu_B}{T}\right) = \frac{1}{T^4}\frac{\partial^n}{\partial(\mu_B/T)^n}P\left(\frac{T}{T_c},\frac{\mu_B}{T}\right)\Bigg|_{T/T_c} \quad (1)$$

Lattice measurements of the series expansion of the NLS in powers of μ_B/T are resummed by using Padé approximants in order to give predictions for the above quantities (*18*). They are of interest because they are related to cumulants of the fluctuations of the baryon number in thermal and chemical equilibrium in a grand canonical ensemble.

The nth cumulant of such fluctuations, $[B^n]$, is given by

$$[B^n] = VT^3T^{n-4}\chi_B^{(n)}\left(\frac{T}{T_c},\frac{\mu_B}{T}\right) \quad (2)$$

where V is the volume of the observed part of the fireball. Because observed hadrons are in thermal and chemical equilibrium at the freeze-out, this relation should hold for cumulants of the observed event-by-event distribution of net-baryon number in heavy ion collisions. The cumulants are often reported as the variance $\sigma^2 = [B^2]$, the skewness $S = [B^3]/[B^2]^{3/2}$, and the Kurtosis $\kappa = [B^4]/[B^2]^2$. It is clear from these definitions that the V-dependence in Eq. 2 gives the correct volume scaling expected from the central limit theorem. This leads to the classic extraction of the susceptibility from fluctuations in the grand canonical ensemble (*27*, *28*).

There is one remaining subtlety in comparing lattice computations with experimental data. Most experiments are designed to measure event-by-event net-protons. The data discussed in the current work is from the STAR experiment at RHIC (*19*), which identifies protons and anti-protons by measuring the specific ionization energy loss of these particles in the gas of a time projection chamber. These measurements miss neutrons, the other dominant part of the baryon distribution. This may impose limitations on our measurement

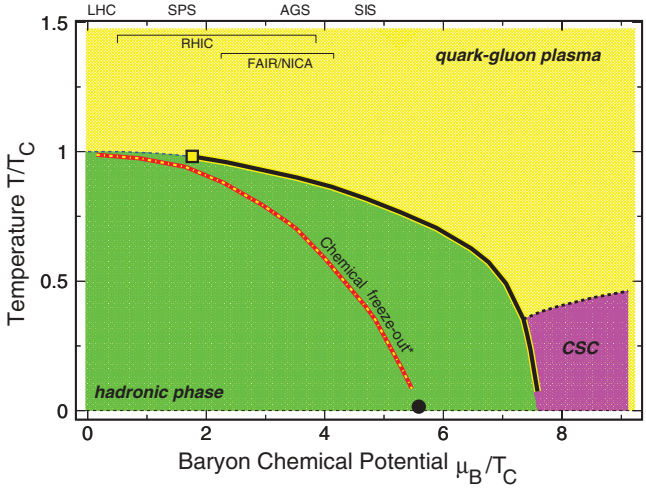

Fig. 2. Current conjectures for the QCD phase diagram. The phase boundary (solid line) between the normal low-temperature hadronic phase of bulk QCD matter and the high-temperature partonic phase is a line of first-order phase transitions that begins at large μ_B and small T and curves toward smaller μ_B and larger T. This line ends at the QCD critical point, whose probable position, derived from lattice computations, is marked by a square. At even smaller μ_B, there are no phase transitions, only a line of cross-overs (dashed line). The red-yellow dotted line corresponds to the chemical freeze-out line from the evolution of the bulk QCD matter produced in high-energy heavy-ion collisions. The solid point at $T = 0$ and μ_B = 938 MeV represents nuclear matter in the ground state. At large μ_B and low T is the color superconductor phase (CSC) (*35*).

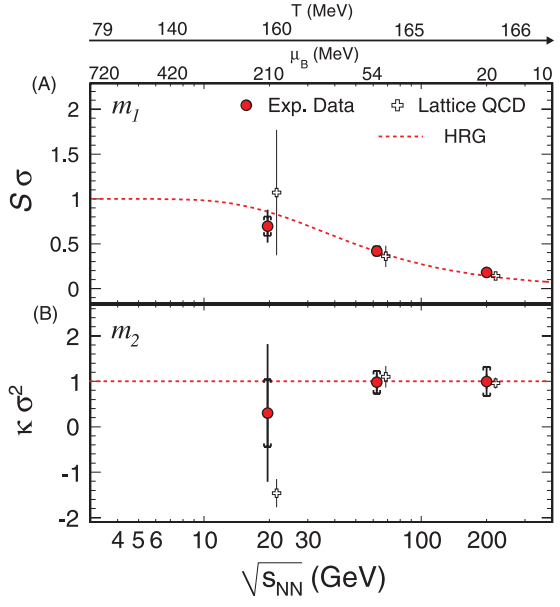

Fig. 3. Comparison of lattice QCD and experimental data for (**A**) m_1 and (**B**) m_2. Experimentally measured ratios of cumulants of net-proton distributions, $m_1 = S\sigma$ and $m_2 = \kappa\sigma^2$, are shown as a function of $\sqrt{s_{NN}}$ for impact parameter values of less than 3 fm for Au+Au collisions at RHIC (*19*). Also plotted on the top scale are the chemical freeze-out values of μ_B and T corresponding to $\sqrt{s_{NN}}$ as obtained from a hadron resonance gas model, which assumes the system to be in chemical and thermal equilibrium at freeze-out (*16*, *17*). The prediction of such a model for m_1 (*33*) is shown as the dashed red line. The lattice predictions for these quantities are drawn from a computation with lattice cutoff of $1/a \cong 960$ to 1000 MeV and converted to the dimensional scale of T and μ by using T_c = 175 MeV.

of fluctuations. However, the effect of isospin fluctuations on the shape of the net-baryon distributions is small (*29*). Hence, we proceeded under the assumption that the shape of the net-proton distributions reflects the net-baryon distributions up to distortions smaller than the estimated errors in measurements of the cumulants.

We are unable to exploit Eq. 2 directly in heavy-ion experiments because the volume, V, is hard to determine precisely experimentally. However, the ratios

$$(m_1): S\sigma = \frac{[B^3]}{[B^2]} = \frac{T\chi_B^{(3)}}{\chi_B^{(2)}},$$
$$(m_2): \kappa\sigma^2 = \frac{[B^4]}{[B^2]} = \frac{T^2\chi_B^{(4)}}{\chi_B^{(2)}},$$
$$(m_3): \frac{\kappa\sigma}{S} = \frac{[B^4]}{[B^3]} = \frac{T\chi_B^{(4)}}{\chi_B^{(3)}} \qquad (3)$$

do not contain the volume and therefore provide a direct and convenient comparison of experiment and theory (*30*). The above equations are written in a form that emphasizes this connection: The left hand side can be measured in an experiment, whereas the right hand side can be predicted with lattice QCD. We use the notation $m_{1,2,3}$ generically to refer to either side.

We now discuss the comparison of m_1 and m_2 from experiment and theory (Fig. 3). The experimental measurements (*19*) were made by using the number of protons (p) and anti-protons ($-p$) produced in the collision of Au ions around 90° to the beam axis with the impact parameter of the collisions being less than 3 fm (*31*). p and $-p$ are in the range of 400 MeV/c to 800 MeV/c, where c is the speed of light. This choice of momentum range is designed to obtain the purest sample of p and $\bar{p}$. A large fraction of p and $\bar{p}$ is contained in this kinematic range. The effect of finite reconstruction efficiency of p and $\bar{p}$ has been shown to be negligible (*19*). The experimental values of $S\sigma$ and $\kappa\sigma^2$ are shown as a function of $\sqrt{s_{NN}}$.

The lattice calculations (*18*) were carried out by using two flavors of staggered quarks in QCD. The lattice cutoff $1/a \cong 960$ to 1000 MeV and the bare quark mass were tuned to give a pion mass of about 230 MeV (*32*). These computations were performed at $\mu_B = 0$, and the Taylor series coefficients of P/T^4 were used to extrapolate m_1 and m_2 to the freeze-out conditions by using appropriate order Padé approximants to resum the series expansions. Because lattice results are obtained in terms of T/T_c and μ_B/T (Eq. 1), their extrapolation to the freeze-out conditions required the input of T_c. The lattice values were obtained by using T_c = 175 MeV, which is compatible with indirect determinations of T_c (*10*–*13*).

On the upper scales of Fig. 3, we also show the μ_B and T values at chemical freeze-out that correspond to the various $\sqrt{s_{NN}}$. For this, we used the functional relationship between these values from the hadron resonance gas model using the yields of hadrons discussed in (*16*, *17*). The model predictions for m_1 (*33*) are also shown. The hadron resonance gas model predictions can be reproduced if baryon and anti-baryon numbers are independently Poisson distributed. Having established a connection between $\sqrt{s_{NN}}$ and (T, μ_B), we compare the experimental data on fluctuations with those predicted from lattice QCD. Excellent agreement is seen between lattice QCD predictions and experimental measurements for all three beam energies. This marks the first successful direct test of QCD against experimental data in the nonperturbative context of bulk hadronic matter. The agreement with the data are yet another nontrivial indication that the fireball produced in heavy ion collisions is in thermal and chemical equilibrium at chemical freeze-out.

Setting the scale of bulk QCD. Lattice QCD results for $m_{1,2,3}$ are obtained for dimensionless arguments T/T_c and μ_B/T, as shown in Eq. 2. For a given value of $\sqrt{s_{NN}}$, the experimental observations are realized at the corresponding chemical freeze-out, characterized by T and μ_B. Thus, a comparison of the two requires a choice of the scale, T_c. By varying this scale to obtain the best fit between the QCD predictions and experimental measurements, we determined T_c for the first time through an observable connected to strongly interacting bulk matter. The results are, of course, subject to all the caveats expressed in the previous section. The observable that we choose for comparison is m_3. The lattice computation of this quantity has the smallest systematic uncertainties among the three explored here and thus is the best quantity to use to constrain T_c.

The comparison of m_3 between experimental results from Au ion collisions and lattice QCD predictions is shown in Fig. 4A. This is an extension of Fig. 3, which shows a comparison with m_1 and m_2. In this analysis, the results of m_1, m_2, and m_3 are consistent, as required in Eq. 3. The new information here is that we show lattice predictions obtained with different values of T_c. The errors on the experimental data points are statistical (lines) and systematic (brackets) errors (*19*). The errors bars on the lattice predictions are statistical errors, with a cutoff of $1/a \cong 960$ to 1000 MeV. The lattice spacing effects and the effect of tuning the bare quark mass are the main sources of remaining uncertainties in the predictions. These are not parameterized as systematic uncertainties. However, it is known that their effect is small at the two highest values of $\sqrt{s_{NN}}$ (*18*).

In order to arrive at a quantitative estimate of the scale parameter T_c, we perform a standard statistical analysis. For each value of T_c, we compute

$$\chi^2(T_c) = \sum_{\sqrt{s_{NN}}} \frac{\left[m_3^{\text{expt}}(\sqrt{s_{NN}}) - m_3^{\text{QCD}}(\sqrt{s_{NN}}, T_c)\right]^2}{Error^2_{\text{expt}} + Error^2_{\text{QCD}}} \qquad (4)$$

where the errors in the experimental and lattice QCD quantities are obtained as explained above. The lattice predictions are calculated for the grid of T_c values (Fig. 4). The minimum of χ^2, corresponding to the most probable value of the parameter being estimated, occurs at T_c = 175 MeV. The standard errors on the parameter are the values of T_c for which χ^2 exceeds the minimum value by unity. It is clear from Fig. 4B that this is bounded by +5 and −10 MeV. A piecewise linear interpolation between the grid points yields the more reliable error estimate, +1 and −7 MeV. By comparing different interpolation schemes, we found that the error estimate is stable. As a result, we conclude that

$$T_c = 175^{+1}_{-7}\ \text{MeV}. \qquad (5)$$

The error estimates include systematic and statistical errors on experimental data but only statistical errors on the lattice QCD computations.

The result in Eq. 5 is compatible with current indirect estimates of T_c that come from setting the

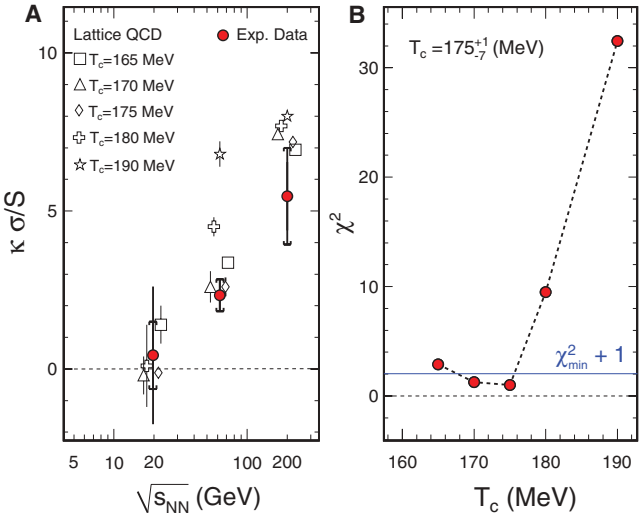

Fig. 4. Comparison of m_3 from experiment and lattice predictions, and the extraction of T_c. (**A**) $\kappa\sigma/S$ of net-proton distribution measured in collisions of Au ions at varying $\sqrt{s_{NN}}$ and with an impact parameter of less than 3 fm. This is compared with lattice QCD predictions with cutoff $1/a \cong 960$ to 1000 MeV for the corresponding ratio of susceptibilities extrapolated to the freeze-out conditions by using different values of T_c. The lattice results at each $\sqrt{s_{NN}}$ are slightly shifted for clarity in presentation. (**B**) The comparison of experimental data and lattice QCD predictions, shown through χ^2 as a function of T_c by using the definition given in Eq. 4. This yields the estimate of T_c, and its errors are as discussed in the text.

scale of thermal lattice QCD computations via hadronic observables. Furthermore, this gives a scale for temperatures that is compatible with the resonance gas model, as shown in Fig. 3. As we discussed in the introduction, this closes a circle of inferences that shows that phenomena obtained in heavy ion collisions are fully compatible with hadron phenomenology and provides a first check in bulk hot and dense matter for the standard model of particle physics.

Conclusions and outlook. We have performed a direct comparison between experimental data from high-energy heavy ion collisions on net-proton number distributions and lattice QCD calculations of net-baryon number susceptibilities. The agreement between experimental data, lattice calculations, and a hadron resonance gas model indicates that the system produced in heavy ion collisions attained thermalization during its evolution. The comparison further enables us to set the scale for nonperturbative, high-temperature lattice QCD by determining the critical temperature for the QCD phase transition to be 175^{+1}_{-7} MeV.

This work reveals the rich possibilities that exist for a comparative study between theory and experiment of QCD thermodynamics and phase structure. In particular, the current work can be extended to the search for a critical point. In a thermal system, the correlation length (ξ) diverges at the critical point. ξ is related to various moments of the distributions of conserved quantities, such as net-baryons, net-charge, and net-strangeness. Finite size and dynamical effects in heavy ion collisions put constraints on the values of ξ (*34*). The lattice calculations discussed here and several QCD-based models have shown that moments of net-baryon distributions are related to baryon number susceptibilities and that the ratio of cumulants $m_2 = \kappa\sigma^2$, which is related to the ratio of fourth-order to second-order susceptibilities, shows a large deviation from unity near the critical point. Experimentally, $\kappa\sigma^2$ can be measured as a function of $\sqrt{s_{NN}}$ (or T and μ_B) in heavy ion collisions. A nonmonotonic variation of $\kappa\sigma^2$ as a function of $\sqrt{s_{NN}}$ would indicate that the system has evolved in the vicinity of the critical point and thus could be taken as evidence for the existence of a critical point in the QCD phase diagram.

References and Notes

1. F. Wilczek, *Phys. Today* **52N11**, 11 (1999).
2. F. Wilczek, *Phys. Today* **53N1**, 13 (2000).
3. G. Sterman *et al*., *Rev. Mod. Phys.* **67**, 157 (1995).
4. M. Peardon, V. Crede, P. Eugenio, A. Ostrovidov, *AIP Conf. Proc.* **1257**, 19 (2010).
5. I. Arsene *et al*., *Nucl. Phys. A* **757**, 1 (2005).
6. B. B. Back *et al*., *Nucl. Phys. A* **757**, 28 (2005).
7. J. Adams *et al*., *Nucl. Phys. A* **757**, 102 (2005).
8. K. Adcox *et al*., *Nucl. Phys. A* **757**, 184 (2005).
9. B. I. Abelev *et al*., *Phys. Rev. C* **79**, 034909 (2009).
10. S. Borsanyi *et al*., *J. High Energy Phys.* **1009**, 073 (2009).
11. Y. Aoki, Z. Fodor, S. Katz, K. Szabo, *Phys. Lett. B* **643**, 46 (2006).
12. M. Cheng *et al*., *Phys. Rev. D* **74**, 054507 (2006).
13. C. Schmidt, paper presented at Quark Confinement and the Hadron Spectrum IX, 30 August 30 to 3 September 2010, Madrid, Spain; available at http://arxiv.org/abs/1012.2230v1.
14. F. R. Brown, N. H. Christ, Y. F. Deng, M. S. Gao, T. J. Woch, *Phys. Rev. Lett.* **61**, 2058 (1988).
15. Y. Aoki, G. Endrodi, Z. Fodor, S. D. Katz, K. K. Szabó, *Nature* **443**, 675 (2006).
16. P. Braun-Munzinger, J. Wambach, *Rev. Mod. Phys.* **81**, 1031 (2009).
17. J. Cleymans, K. Redlich, *Phys. Rev. Lett.* **81**, 5284 (1998).
18. R. V. Gavai, S. Gupta, *Phys. Lett. B* **696**, 459 (2011).
19. M. M. Aggarwal *et al*., *Phys. Rev. Lett.* **105**, 022302 (2010).
20. M. A. Stephanov, K. Rajagopal, E. V. Shuryak, *Phys. Rev. D* **60**, 114028 (1999).
21. R. D. Pisarski, F. Wilczek, *Phys. Rev. D* **20**, 338 (1984).
22. S. Gupta, *PoS* **LATTICE2010**, 007 (2010).
23. B. I. Abelev *et al*., *Phys. Rev. C* **81**, 024911 (2010).
24. B. Mohanty, *Nucl. Phys. A.* **830**, 899c (2009).
25. μ_B of bulk nuclear matter is quoted in the usual convention adopted in relativistic treatments because anti-baryon production also needs to be accounted for. An alternative (nonrelativistic) definition that takes nucleon number to be fixed would give much smaller chemical potential. However, this does not correspond to the physics of baryon number fluctuations that we examine.
26. R. V. Gavai, S. Gupta, *Phys. Rev. D* **68**, 034506 (2003).
27. M. Asakawa, U. Heinz, B. Muller, *Phys. Rev. Lett.* **85**, 2072 (2000).
28. S. Jeon, V. Koch V, *Phys. Rev. Lett.* **85**, 2076 (2000).
29. Y. Hatta, M. A. Stephanov, *Phys. Rev. Lett.* **91**, 102003 (2003).
30. S. Gupta, *PoS* **CPOD2009**, 25 (2009).
31. The impact parameter is determined through a Glauber Monte Carlo procedure. The selected events correspond to the most central 0 to 5% and 0 to 10% events of the total hadronic cross section in Au+Au collisions for $\sqrt{s_{NN}}$ = 200, 62.4, and 19.6 GeV, respectively.
32. The change in the radius of convergence in going from $m_\pi/m_\rho = 0.33$ to 0.2 is likely to be between 10 and 15% (*22*). The corresponding effect on m_3 is about 2% or less at the two highest energies and less than 20% at an energy of 19.6 GeV.
33. F. Karsch, K. Redlich, *Phys. Lett. B* **695**, 136 (2011).
34. B. Berdnikov, K. Rajagopal, *Phys. Rev. D Part. Fields* **61**, 105017 (2000).
35. M. G. Alford, K. Rajagopal, F. Wilczek, *Phys. Lett. B* **422**, 247 (1998).

Acknowledgments: We thank Z. Fodor, R. V. Gavai, F. Karsch, D. Keane, V. Koch, B. Mueller, K. Rajagopal, K. Redlich, H. Satz, and M. Stephanov for enlightening discussions. We acknowledge the Indian Lattice Gauge Theory Initiative for computational support, the Department of Atomic Energy–Board of Research in Nuclear Sciences through the project sanction 2010/21/15-BRNS/2026, the U.S. Department of Energy under contract DE-AC03-76SF00098, and the Chinese Ministry of Education.

21 February 2011; accepted 4 May 2011
10.1126/science.1204621

The Oxygen Isotopic Composition of the Sun Inferred from Captured Solar Wind

K. D. McKeegan,[1*] A. P. A. Kallio,[1] V. S. Heber,[1] G. Jarzebinski,[1] P. H. Mao,[1,2] C. D. Coath,[1,3] T. Kunihiro,[1,4] R. C. Wiens,[5] J. E. Nordholt,[5] R. W. Moses Jr.,[5] D. B. Reisenfeld,[6] A. J. G. Jurewicz,[7] D. S. Burnett[8]

All planetary materials sampled thus far vary in their relative abundance of the major isotope of oxygen, ^{16}O, such that it has not been possible to define a primordial solar system composition. We measured the oxygen isotopic composition of solar wind captured and returned to Earth by NASA's Genesis mission. Our results demonstrate that the Sun is highly enriched in ^{16}O relative to the Earth, Moon, Mars, and bulk meteorites. Because the solar photosphere preserves the average isotopic composition of the solar system for elements heavier than lithium, we conclude that essentially all rocky materials in the inner solar system were enriched in ^{17}O and ^{18}O, relative to ^{16}O, by ~7%, probably via non–mass-dependent chemistry before accretion of the first planetesimals.

The gravitational collapse of a molecular cloud fragment 4.57 billion years ago led to an accretion disc of gas and dust, the solar nebula, from which the Sun and planets formed. This nebula was approximately homogeneous with respect to isotopic abundances, which, given that isotope ratios from various stellar nucleosynthetic processes vary widely, points to efficient mixing either in interstellar space or in the solar nebula. Thus, the discovery (*1*) that high-temperature minerals in carbonaceous chondrite meteorites are enriched preferentially in ^{16}O compared to ^{17}O and ^{18}O relative to the abundances in terrestrial samples was considered evidence for the presence of exotic material that escaped thorough mixing and thereby

[1]Department of Earth and Space Sciences, University of California–Los Angeles (UCLA), Los Angeles, CA 90095–1567, USA. [2]Division of Physics, Math, and Astronomy, California Institute of Technology (Caltech), Pasadena, CA 91125, USA. [3]School of Earth Sciences, University of Bristol, Bristol BS8 1RJ, UK. [4]Institute for Study of the Earth's Interior, Okayama University, Misasa, Tottori 682-0193, Japan. [5]Los Alamos National Laboratory, Los Alamos, NM 87545, USA. [6]Department of Physics and Astronomy, University of Montana, Missoula, MT 59812, USA. [7]Center for Meteorite Studies, Arizona State University, Tempe, AZ 85287, USA. [8]Division of Geological and Planetary Science, Caltech, Pasadena, CA 91125, USA.

*To whom correspondence should be addressed. E-mail: mckeegan@ess.ucla.edu

ERRATUM

Post date 16 September 2011

Research Articles: "Scale for the phase diagram of quantum chromodynamics" by S. Gupta *et al.* (24 June, p. 1525). The corresponding author's e-mail address was incorrect. It should be bmohanty@vecc.gov.in. The address has been corrected in the HTML version online.

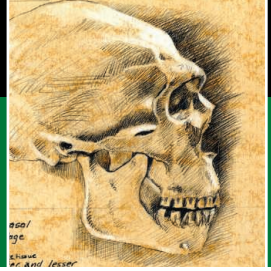

LETTERS

edited by Jennifer Sills

Trade-Secret Model: Privacy Rights

IN THEIR POLICY FORUM "GENOMICS, BIOBANKS, AND THE TRADE-secret model" (15 April, p. 309), R. Mitchell and his colleagues suggest that trade-secret law could be applied effectively to manage the use of human genomic information. It would be productive to assess the potential application of two other legal models as well: the individual's right to control his or her name and likeness, and the right to control public disclosure of private facts.

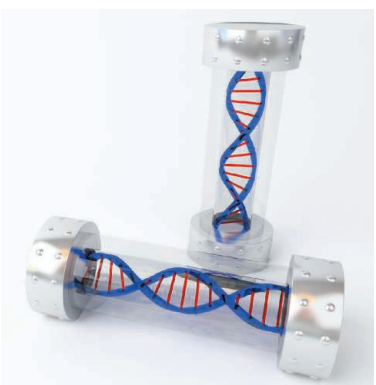

Jurisdictions that recognize a right of personal privacy commonly include within that right the ability of an individual to control the use of his/her name and likeness for commercial advantage (*1*). An individual's name and visual image are deemed to be unique and highly personal qualities that each person should have the right to control. This right is viewed by the law as part of the individual's ability to protect the key aspects of his/her personality. Name and likeness have been interpreted to include other characteristics of an individual's personality, including the sound of his or her voice (*2*). It seems reasonable that the legal framework designed to help the individual to protect the integrity of his/her personality should also include the most intimate aspect of an individual's personality—personal genomic information.

Personal privacy rights also frequently include the ability to control public disclosure of private facts about an individual (*3*). Arguably, genomic information includes the most private and personal facts associated with any individual. The right to control public disclosure of private facts appears to provide another legal vehicle for management of use of personal genomic information.

Application of these traditional privacy rights can supplement legal approaches such as the trade-secret model proposed by Mitchell *et al*. There may also be circumstances in which the trade-secret model would not be appropriate but the traditional privacy rights could be applied. For example, it is unclear whether an individual can effectively assert a trade-secret claim when the secret he or she possesses is not actually understood by the individual asserting the protection. No such complications arise when a traditional personal privacy right is applied.

JEFFREY H. MATSUURA

Alliance Law Group, 7700 Leesburg Pike, Falls Church, VA 22043, USA. E-mail: jmatsuura@alliancelawgroup.com

References

1. California Civil Code, Section 3344.
2. Massachusetts General Laws, Chapter 214, Section 1B.
3. California State Constitution, Article I, Section 1B and Florida State Constitution, Article I, Section 23.

Trade-Secret Model: Potential Pitfalls

IN THEIR POLICY FORUM "GENOMICS, BIOBANKS, and the trade-secret model" (15 April, p. 309), R. Mitchell *et al*. submit that donating genetic samples for medical research is like selling a confidential commodity of potentially lucrative value, warranting individual licensing arrangements to secure acceptable benefit outcomes. We disagree with this approach to building cancer research biorepositories.

Trade secrets derive value from being unknown and not readily ascertainable (*1*). By contrast, the value of human subject biospecimens contributed for cancer research increases with widespread dissemination for use in approved studies, accompanied by open sharing of data. (*2*–*5*). Whereas trade-secret doctrine recognizes the necessity of preserving confidential information to further personal gain, research participants contributing samples and associated data are primarily motivated by altruistic, not compensatory, desires (*2*, *3*, *6*, *7*).

Moreover, the trade-secret model is not practical from the perspective of biobanking operations and governance. How might cancer biorepositories accurately track and implement the diverse licensing preferences of multiple research participants with respect to such issues as determining future research uses of biospecimens, or returning research results? What if participants wanted to negotiate profit distributions for successful products developed in part based on their contributions? How can the numerous, incremental research advances that precede product development be quantified in order to determine a fair distribution of commercial profits among research participants? Progress in scientific research, particularly in the accelerating world of cancer genomics, is not typically attributed to single biospecimen contributors [Henrietta Lacks (*8*) notwithstanding]. Heralded by the authors as furthering individual autonomy, the trade-secret model has the potential to foment suspicion and distrust among research participants as they compete for the highest-profit dividends.

Published by AAAS

Pulling off difficult reactions

1582

Feather evolution

1590

In lieu of evaluating the biospecimen contributions of cancer research participants under a trade-secret model, we advocate a custodianship model as set forth in the National Cancer Institute's Best Practices for Biospecimen Resources (*9*). The custodianship model supposes that biorepositories accept responsibility for ensuring the long-term quality and security of contributed biospecimens and protect the confidentiality of participant data. This model promotes equitable and continuous access to biospecimens for research in accordance with scientifically vetted public priorities, maintaining trust through accountability, transparency, and justice (*10*).

CAROL J. WEIL AND CAROLYN COMPTON

Office of Biorepositories and Biospecimen Research, Center for Strategic Scientific Initiatives, The National Cancer Institute, National Institutes of Health, Bethesda, MD 20892, USA.

*To whom correspondence should be addressed. E-mail: carol.weil@nih.gov

References and Notes

1. U.S. National Conference of Commissioners on Uniform State Laws, *Uniform Trade Secrets Act*, §1(4).
2. C. Galbraith, *Miss. Law J.* **78**, 705 (2009).
3. J. Drazen, A. Wood, *N. Engl. J. Med.* **353**, 2809 (2005).
4. NIH, Policy for Sharing of Data Obtained in NIH Supported or Conducted Genome-Wide Association Studies (GWAS) (http://grants.nih.gov/grants/guide/notice-files/NOT-OD-07-088.html).
5. International Network of Cancer Genome Projects, *Nature* **464**, 993 (2010).
6. J. Thornton, *Int. J. Surg.* **7**, 501 (2009).
7. L. Beskow, E. Dean, *Cancer Epidemiol. Biomarkers Prev.* **17**, 1440 (2008).
8. R. Skloot, *The Immortal Life of Henrietta Lacks* (Crown, New York, 2010).
9. National Cancer Institute, Office of Biorepositories and Biospecimen, 2010 Revised NCI Best Practices (http://biospecimens.cancer.gov/practices/2010bp.asp).
10. Custodianship and Ownership Issues in Biospecimen Research Symposium/Workshop, Rockville, MD, 4 to 5 October 2007; http://biospecimens.cancer.gov/global/pdfs/CaOSumm.pdf.

Letters to the Editor

Letters (~300 words) discuss material published in *Science* in the past 3 months or matters of general interest. Letters are not acknowledged upon receipt. Whether published in full or in part, Letters are subject to editing for clarity and space. Letters submitted, published, or posted elsewhere, in print or online, will be disqualified. To submit a Letter, go to www.submit2science.org.

Trade-Secret Model: Legal Limitations

THE POLICY FORUM "GENOMICS, BIOBANKS, and the trade-secret model" (R. Mitchell *et al.*, 15 April, p. 309) introduces a new way to promote the autonomy of research participants in genomic biobanks. However, the proposed trade-secret model suffers from socio-ethical and legal flaws.

First, Mitchell *et al.* conflate the "value" of an individual's genetic information with a "secret." Rather than articulating a case for such a link, the authors simply posit that "information encoded by an individual's DNA" is "something of unique value for a certain kind of 'business' (biomedical research)." However, unique values do not necessarily have to be secrets.

Second, the trade-secret model will diminish, not enhance, the autonomy of research participants. Enabling biobank contributors to obtain legal ownership (not mere possession) of their genetic information and set the parameters of its use will not permit them greater self-control, free from external interference. Rather, participants will be subjected to contractual negotiations with biobankers. Because the biobankers will unilaterally draft the "limited menu of options," the trade-secret model could increase the possibility of a power imbalance (*1*).

Third, the model contains legal and policy flaws. Trade-secret information, by definition, must confer an economic benefit on the holder, deriving specifically from the fact that the information is not generally known (*2*, *3*). Genetic information is financially worthless absent outsourced scientific interpretation and technological application (and even then, there is no guarantee of its financial worth). Trade secrets presuppose that the holder knows the confidential information; here, individuals do not know most of their own genetic information, but the researcher will (*4*). Also, trade secrets do not ameliorate power balance, autonomy, or compensation issues. They are not instrumental legal tools to serve (bio)ethical ends. They are solely means to obtain an economic advantage over others. Do we want to foster a research environment in which biobankers and contributors compete against each other to obtain the most favorable economic terms?

Ultimately, to reap the promised medical benefits of genomic research for all of society, we must eschew the individualistic, procedural vision of research that falsely assumes all actors possess conflicting agendas irrevocably irreconcilable outside a legal forum. We should focus instead on developing robust, transparent, and collaborative research models that will truly benefit humanity (*5*).

EDWARD S. DOVE, YANN JOLY,* BARTHA M. KNOPPERS

Centre of Genomics and Policy, Department of Human Genetics, McGill University, Montreal, QC, H3A 1A4, Canada.

*To whom correspondence should be addressed. E-mail: yann.joly@mail.mcgill.ca

References

1. L. Mulcahy, J. Tillotson, *Contract Law in Perspective* (Cavendish, London, ed. 4, 2004).
2. U.S. National Conference of Commissioners on Uniform State Laws, *Uniform Trade Secrets Act*, § 1(4).
3. American Law Institute, *Restatement of the Law (Third), Unfair Competition*, § 39.
4. J. Couzin-Frankel, *Science* **331**, 662 (2011).
5. B. M. Knoppers, Y. Joly, *Trends Biotechnol.* **25**, 284 (2007).

Response

IN OUR POLICY FORUM, WE PROPOSED A trade-secret model that would enable greater autonomy for individuals who contribute to genomic biobanks by contesting elements of the informed consent regime. We thank Matsuura, Weil and Compton, and Dove, Joly, and Knoppers for their thoughts on the potential of this model.

Matsuura proposes that personal privacy rights could strengthen recognition of research participant autonomy. Personal privacy rights enable individuals to control public use of personal or private information or characteristics, and are thus a solution to the problem of unwanted public disclosure. Yet whether guided by current human subjects research protections or recent exemption guidelines, researchers generally promise not to make public any link between individuals and their DNA. Our proposal aims to enhance participant autonomy whether or not unwanted public disclosure becomes an issue.

Our model does not require that individuals understand their secret, as both Matsuura and Dove, Joly, and Knoppers suggest. The information qualifies as long as it "derives economic value, actual or potential, from not being generally known" (*1*).

We do not oppose the custodianship model advocated by Weil and Compton, although we find it legally complex and indeterminate. We do disagree, however, with several of their claims. We do not "submit that donating genetic samples for medical research is like selling a confidential commodity of potentially lucrative value." Rather, we believe that prospective participants view their DNA as confidential property, and often consider the terms and conditions—which may include financial compensation—upon which they might permit its use. Likening a participant's DNA to a trade secret does not imply that its primary value is personal gain, nor does it preclude "widespread dissemination for use." On the contrary, the licensing of trade secrets often encourages widespread dissemination. Researchers working on "approved studies" can, if inclined, include in their menu options a provision for open sharing.

With respect to practicalities, we do not propose recognizing the "diverse licensing preferences" of participants. We propose that biobanks offer participants a limited menu of licenses that differ, for example, in the nature of the compensation and the extent of the permitted use. Just as sharing biospecimens motivated creation of material transfer agreements, licensing needs can drive creative approaches to track permitted options. We also wish to clarify that although Weil and Compton (understandably) refer frequently to cancer research, we think that our model should be tested first among healthy volunteers.

Weil and Compton's claim that our model may "foment suspicion and distrust among research participants" seems inconsistent with their claim that research participants "are primarily motivated by altruistic, not compensatory, desires." Our research suggests that participants are motivated by both altruism and money, with the respective contributions varying among individuals (*2*)—a reality that our model recognizes. We feel that the current interpretation of human subjects regulation is more likely than our proposal to alienate many among the large populations necessary for biobanking, given that informed consent often serves as a quasilegal device to ensure that an institution retains rights to whatever is derived from a biospecimen yet absolves itself of liability. Our model, by contrast, offers a way for individuals to be actual partners, rather than simply "subjects," in biobank research.

Dove, Joly, and Knoppers are concerned that we conflated "value" with "secret." However, we described these terms as the two distinct elements of the legal definition of a trade secret: It must have economic value to its proprietor, and it must not be generally known. The avid interest of medical science in obtaining DNA samples seems to be conclusive evidence that a person's genetic information has economic value. Likewise, it seems self-evident that DNA information cannot be generally known unless and until the person chooses to make it available.

We do not see why a menu of options would in principle promote a power imbalance, as Dove, Joly, and Knoppers suggest, given that a menu could be developed in cooperation with likely participants. Such an imbalance seems more likely in the present system of informed consent. Currently, the prospective participant has two choices—take it or leave it—and all terms are dictated by the researcher, and are probably legally unenforceable by the participant (*3*).

The fact that "genetic information is financially worthless absent outsourced scientific interpretation" is not relevant. Many trade secrets cannot be exploited without third-party expertise and resources—that is why their proprietors license them out.

Finally, Dove, Joly, and Knoppers suggest that increasing contributor autonomy may run counter to "robust, transparent, and collaborative research models." We disagree that autonomy and collaboration are opposed, given that true collaboration seems to require that each participant retain autonomy. The idea that the trade-secret model necessarily facilitates rampant individualism is a misunderstanding of the concept of intellectual property. Contrary to what Dove, Joly, and Knoppers contend, trade secrets—and intellectual property generally—can indeed be "instrumental legal tools to serve (bio)ethical ends." Intellectual property owners use their rights to promote the public interest all the time; for example, PXE International holds and uses a patent (which could just as well be a trade secret) not for profit but to promote its health agenda.

If our proposal were given a trial among healthy volunteers, we suspect that many if not most of them would seek the same eleemosynary ends for which Dove, Joly, and Knoppers argue. However, our proposal would let participants make that choice, rather than deferring to scientific and academic elites who speak for them.

ROBERT MITCHELL,[1] JOHN M. CONLEY,[2] ARLENE M. DAVIS,[2] R. JEAN CADIGAN,[2] ALLISON W. DOBSON,[2] RYAN Q. GLADDEN[2]

[1]Institute for Genome Sciences and Policy and English Department, Duke University, Durham, NC 27708, USA. [2]School of Law, Department of Social Medicine, and Center for Genomics and Society, University of North Carolina, Chapel Hill, NC 27599–3380, USA.

*To whom correspondence should be addressed. E-mail: rmitch@duke.edu

References

1. U.S. National Conference of Commissioners on Uniform State Laws, *Uniform Trade Secrets Act*, § 1(4).
2. R. J. Cadigan, A. M. Davis, in *Governing Biobanks*, J. Kaye, M. Stranger, Eds. (Ashgate Publishing, Farnham, UK, 2009), pp. 117–133.
3. Greenberg v. Miami Children's Hospital Research Institute, 264 F. Supp. 2d 1064 (S.D. Fla. 2003).

CORRECTIONS AND CLARIFICATIONS

Reports: "Adipose triglyceride lipase contributes to cancer-associated cachexia" by S. K. Das *et al*. (8 July, p. 233). Fig. 1G shows normalized white adipose tissue (WAT) weight of gonadal, retroperitoneal, and visceral WAT. In Fig. 1, G to J, descriptions of "epididymal WAT" actually refer to retroperitoneal WAT. In addition, the last complete sentence on p. 235 should read, "To assess the contribution of adipose tissue loss to the tumor-induced weight loss, we determined white adipose tissue (WAT) mass by visual inspection, weighing surgically removed adipose depots (gonadal, retroperitoneal, and visceral adipose tissue) and in vivo nuclear magnetic resonance (NMR) WAT quantitation."

Research Articles: "Scale for the phase diagram of quantum chromodynamics" by S. Gupta *et al*. (24 June, p. 1525). The corresponding author's e-mail address was incorrect. It should be bmohanty@vecc.gov.in. The address has been corrected in the HTML version online.

TECHNICAL COMMENT ABSTRACTS

Comment on "A Test of the Snowball Theory for the Rate of Evolution of Hybrid Incompatibilities"

Daniel A. Barbash

Matute *et al*. (Reports, 17 September 2010, p. 1518) tested the theory that the number of genes involved in hybrid incompatibility increases faster than linearly. However, the method they used is inappropriate because it detects genes that are haploinsufficient in a hybrid background but that would not contribute to lethality in wild-type hybrids, thus overestimating the frequency of hybrid inviability.

Full text at www.sciencemag.org/cgi/content/full/333/6049/1576-b

Response to Comment on "A Test of the Snowball Theory for the Rate of Evolution of Hybrid Incompatibilities"

Daniel R. Matute, David A. Turissini, Jerry A. Coyne

Barbash claims that deficiency mapping of inviability regions cannot distinguish hybrid lethality from haploinsufficiency, the phenomenon whereby a single functional copy of a gene cannot maintain normal function in a hybrid genetic background. Although we acknowledge that his hypothesis deserves careful experimental testing, we argue against his conclusions and provide evidence that our methodology is suitable to study the evolution of Dobzhansky-Muller incompatibilities.

Full text at www.sciencemag.org/cgi/content/full/333/6049/1576-c